

Involvement of Clathrin-Mediated Endocytosis in Human Immunodeficiency Virus Type 1 Entry

Jessica Daecke, Oliver T. Fackler, Matthias T. Dittmar,
and Hans-Georg Kräusslich*

Abteilung Virologie, Universitätsklinikum Heidelberg, D-69120 Heidelberg, Germany

Received 1 June 2004/Accepted 3 September 2004

Productive entry of human immunodeficiency virus (HIV) is believed to occur by direct fusion at the plasma membrane. Endocytic uptake of HIV particles has been observed in several studies but is considered to be nonproductive, leading to virus degradation in the lysosome. We show here that endocytosis contributes significantly to productive HIV entry in HeLa cells by using *trans* dominant-negative mutants of dynamin and Eps15. Inducible expression of a dominant-negative mutant of dynamin in a CD4-positive HeLa cell line reduced HIV infection by 40 to 80%. This effect was independent of the infectious dose and was observed for three different isolates. Analysis of reverse transcription products by real-time PCR and of virus entry by delivery of a virion-associated Vpr- β -lactamase fusion protein revealed a similar reduction, indicating that the block occurred at the entry stage. A strong reduction of HIV entry was also observed upon transient transfection of a different *trans* dominant-negative variant of dynamin, and this reduction correlated with the relative inhibition of transferrin endocytosis. Expression of a dominant-negative variant of Eps15, which is specific for clathrin-dependent endocytosis, reduced HIV entry in HeLa cells by ca 95%, confirming the role of endocytosis for productive infection. In contrast, no effect was observed for a dominant-negative variant of caveolin. We conclude that dynamin-dependent, clathrin-mediated endocytosis can lead to productive entry of HIV in HeLa cells, suggesting this pathway as an alternative route of virus entry.

The first, essential step for a mammalian virus to initiate a successful infection is to overcome the membrane barrier of the host cell, which separates it from the reproduction machinery located in the cytosol or nucleus. Enveloped viruses release their genome into the cytoplasm by fusing the viral envelope with the host membrane, which is initiated by interaction of viral fusion proteins with cellular receptors. Some viruses, such as influenza virus (44, 56) and vesicular stomatitis virus (VSV) (36), need an acidified environment to activate their fusion proteins, and these pH-dependent viruses require internalization by endocytic vesicles to reach the cytosol. Other viruses, such as herpesviruses, are not dependent on low-pH activation and enter the cytosol directly by fusion at the plasma membrane (30), at least in certain cell lines (41). A third mode of entry was recently defined for simian virus 40 (SV40) that is internalized via caveolar vesicles without passing an acidified environment (48, 49).

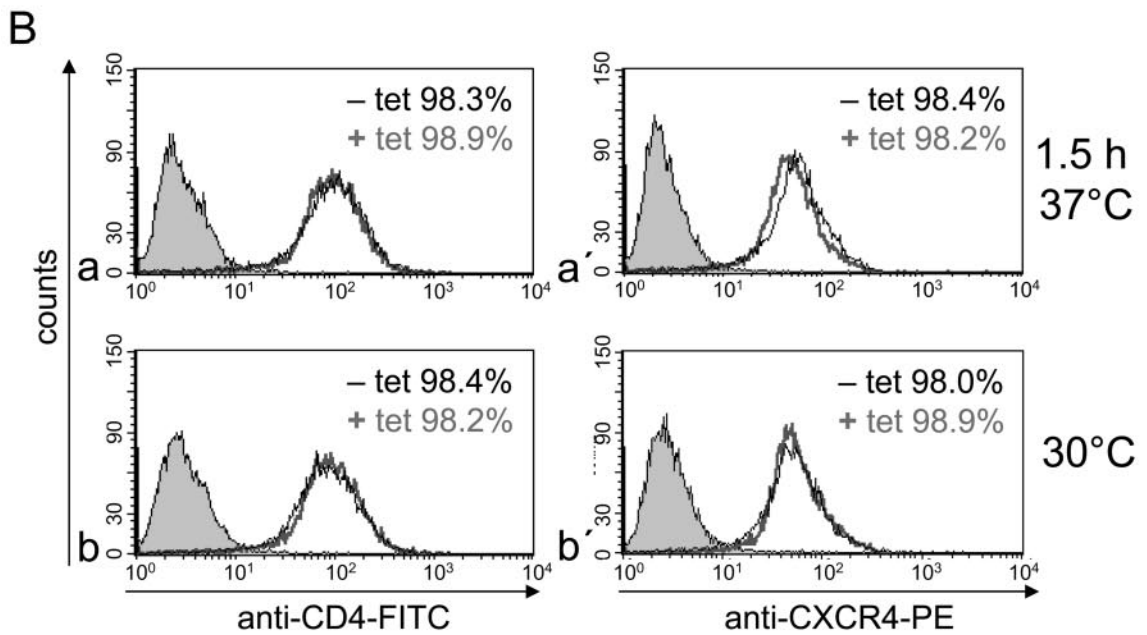
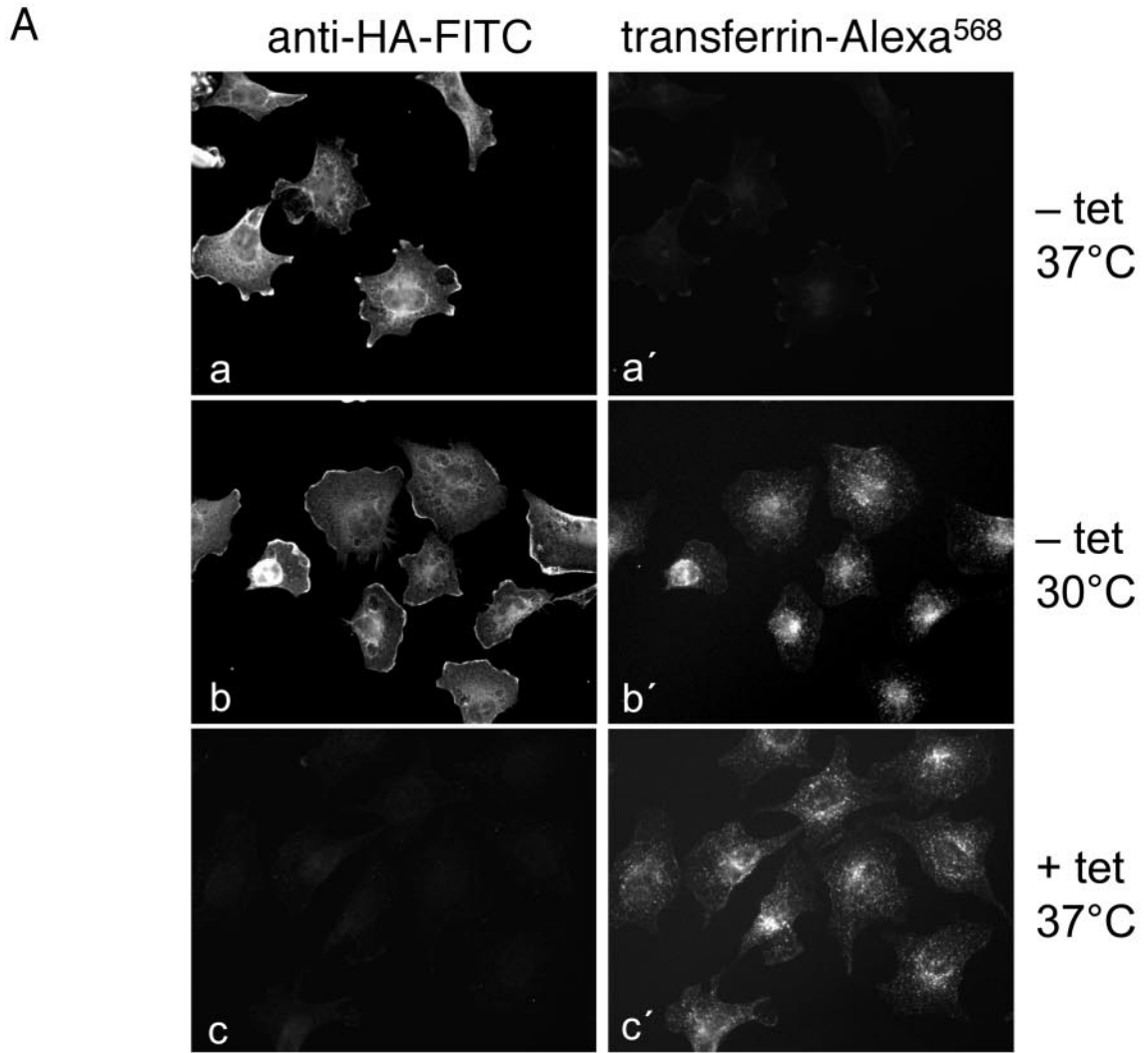
Until recently, entry of retroviruses was believed to occur exclusively at the plasma membrane in a pH-independent manner. This was largely based on experiments with inhibitors of endosomal acidification showing no effect on retroviral infection (2, 17, 35, 58). However, inhibitory effects of agents interfering with endosomal acidification may be transient, and the outcome of such experiments can be influenced by the stability of the viral particle. Indeed, entry of avian leukosis virus was subsequently shown to require endosomal entry and acidification after receptor engagement, which had not been detected

previously because of high particle stability (39). Recently, endocytosis was also suggested to be important for cytosolic entry of amphotropic and ecotropic murine leukemia viruses (27).

Since lysosomotropic agents did not decrease infection, productive entry of human immunodeficiency virus type 1 (HIV-1) is believed not to require acidification and has generally been assumed to take place at the plasma membrane (37, 58). However, nonspecific vesicular internalization of HIV-1 particles can be readily observed in cells independently of expression of the primary entry receptor CD4. Despite internalization of virions, productive infection of CD4-negative cells was not detected by cell fractionation (33) and electron microscopic studies (23, 24). Furthermore, the presence of CD4 and a coreceptor at the cell surface has been shown to be a prerequisite for cytoplasmic entry of HIV-1 (18, 51), and HIV-1 readily infects cells expressing internalization-deficient mutants of CD4 or CCR5 (7, 46). Endocytic uptake of HIV-1, which is frequently observed, is therefore generally judged as a dead end for productive infection.

Although most particles internalized by the vesicular pathway appear to be degraded in the lysosome, there is no direct evidence that escape from vesicles into the cytosol via receptor-mediated fusion does not occur. The gradual pH decrease in the lumen of endocytotic vesicles may permit escape to the cytoplasm for at least some HIV-1 particles prior to damage of the particle by strong acidification. Recent studies demonstrated that endocytic entry by HIV-1 can indeed be productive depending on the experimental conditions, target cells, and viral isolates used (19, 21, 34, 52). For example, inhibition of acidification has been shown to enhance HIV-1 infectivity, presumably by blocking endosomal or lysosomal degradation

* Corresponding author. Mailing address: Abteilung Virologie, Universitätsklinikum Heidelberg, Im Neuenheimer Feld 324, D-69120 Heidelberg, Germany. Phone: 49-6221-56-5001. Fax: 49-6221-56-5003. E-mail: Hans-Georg_Krausslich@med.uni-heidelberg.de.



(21). Moreover, HIV-1 particles were detected in macropinosomes upon infection of macrophages and in this cell type vesicular uptake and access to the cytosol were inhibited by dimethyl amiloride, an inhibitor of macropinocytosis (34).

Distinct cellular structures such as caveolae, clathrin-coated pits, macropinosomes, and phagosomes are utilized by different viruses for endocytic entry (reviewed in reference 47). The cellular GTPase dynamin is essential for clathrin-mediated and caveolar transport (26, 43, 54), whereas fluid-phase uptake is not inhibited by dynamin mutants (14, 15). Mutant dynamin molecules have been useful for the study of entry pathways of different viruses and for the characterization of the endocytic route (48, 49, 57). Dynamin is a 100-kDa GTPase that mediates the release of dynamin-dependent endocytic vesicles from the plasma membrane. *trans* dominant-negative dynamin mutants contain point mutations that affect either their ability to hydrolyze GTP in a temperature-dependent manner ($\text{dyn}^{\text{G273D}}$ or dyn^{ts}) or their affinity for GTP (dyn^{K44A}). Both dynamin variants prevent the pinching off of endocytic vesicles from the inner leaflet of the plasma membrane. Dynamin might also play a role in phagocytosis (22), whereas its function in macropinosomal transport is controversial and may depend on experimental conditions (38, 53). Dominant-negative dynamin interferes with several endocytic routes and specific inhibition of either clathrin-mediated endocytosis or caveolar uptake can be achieved by other *trans* dominant-negative proteins exclusively affecting one of these pathways. A dominant-negative variant of Eps15, an interaction partner of the AP2 complex, inhibited clathrin-mediated endocytosis specifically and blocked Sindbis virus, Semliki Forest virus, and adenovirus infection (reviewed in reference 55). A green fluorescent protein (GFP)-caveolin fusion protein, on the other hand, selectively interfered with SV40 uptake by caveolae (48, 49).

We characterized here the role of endocytic processes for productive entry of HIV-1 by using *trans* dominant-negative mutants of dynamin, Eps15, and caveolin to block endocytosis without interfering with the endosomal pH. Expression of dyn^{ts} in a stably transduced HeLa cell line during the entry phase reduced the number of infected cells, the accumulation of reverse transcription (RT) products, and the cytosolic entry of HIV-1 by 40 to 80%. These effects were observed over a wide range of infectious doses and for various HIV-1 isolates. Cytosolic entry was also strongly inhibited by dyn^{K44A} and dominant-negative Eps15. In contrast, dominant-negative caveolin-1 did not interfere with HIV-1 entry. We conclude that dynamin-dependent, clathrin-mediated uptake can lead to pro-

ductive entry by HIV-1, suggesting this pathway as an alternative route of virus entry to fusion at the plasma membrane.

MATERIALS AND METHODS

Plasmids. Plasmids Eps15GFP (originally named DIIIΔ2) and dnEps15GFP (originally named EΔ95/295) have been described previously (3, 4) and were provided by A. Dautry-Varsat. The caveolin-1 expression plasmid cavGFP (originally named caveolin1-GFP) has been described (48). Plasmid dncavGFP (originally named pINDEGFPVIP) has also been described (32). Mutant dynamin^{K44A} was described by van der Blik et al. (60). Dyn^{wt} GFP (originally named Dyn2-GFP) was described previously (8). CavGFP, dncavGFP, dyn^{wt} -GFP, and dyn^{K44A} GFP were provided by A. Helenius. The expression vector for the fusion protein of β -lactamase and Vpr (pMM310) (59) was a gift from N. Landau. The expression plasmid for the envelope glycoprotein of VSV (VSV-G) under control of the cytomegalovirus promoter (pM3) was provided by D. von Laer. An HIV-1 proviral clone with a deletion of the *env* open reading frame (pNL4-3 env^- GFP) was provided by D. Gabuzda (25).

Cells and tissue culture. HeLa cells, CD4-positive HeLaP4 cells (10), and 293T cells were grown in Dulbecco modified Eagle medium (Gibco) supplemented with 10% heat-inactivated fetal calf serum (FCS), penicillin (100 U/ml), streptomycin (100 $\mu\text{g}/\text{ml}$), and 4 mM glutamine. MT-4 cells were maintained in RPMI 1640 medium supplemented with 10% FCS, penicillin (100 U/ml), streptomycin (100 $\mu\text{g}/\text{ml}$), 4 mM glutamine, and 5 mM HEPES-free acid. All cells were cultivated at 37°C and 5% CO_2 .

The stably transformed tTA-HeLa cells with tightly regulated expression of dyn^{ts} were kindly provided by S. Schmid (13). This cell line expresses a dynamin variant with a point mutation from G to D in position 273 under control of a tetracycline-regulated promoter. The G273D mutation was first discovered in the *Drosophila* mutant *shibire*, which fails to recycle neurotransmitters at the synapse at the nonpermissive temperature (28). The packaging cell line PA317/CD4 releasing amphotropic retrovirus vector particles transducing the human CD4 gene has been described (11) and was provided by P. Clapham. To produce a CD4-positive derivative of dyn^{ts} cells, retrovirus vector particles were harvested from PA317/CD4 cells, filtered, and used to transduce the stably transformed tTA HeLa cells with regulated dyn^{ts} expression in the presence of 8 μl of Polybrene/ml. Cells were cultured in Dulbecco modified Eagle medium with the described supplements and 200 ng of puromycin (Sigma)/ml, 400 μg of Geneticin (Gibco)/ml, 1 μg of tetracycline (tet) (Sigma)/ml, and 1 mM sodium pyruvate. Transduced cells were incubated with CD4 antibodies conjugated to superparamagnetic MicroBeads (Miltenyi Biotec) and CD4-positive cells were preselected by magnetic activated cell sorting. Clonal cell lines were selected by staining with an antibody against CD4 conjugated with fluorescein isothiocyanate (FITC) and sorting of single CD4-positive cells by using a FACSorter. Cell lines were analyzed for expression of CD4 and tet-inducible expression of dyn^{ts} by fluorescence-activated cell sorting (FACS) and immunofluorescence, respectively, resulting in the cell line HeLa4D9.

For single-round entry assays, 3×10^5 HeLa4D9 cells in 10-cm plates were incubated overnight in medium supplemented with 1 μg of tet/ml at 37°C, followed by incubation in the presence or absence of tet for 24 h at 32°C. Subsequently, cells were treated with trypsin and plated according to the type of the experiment (1.1×10^4 cells per 48 wells for analysis of viral capsid [CA] expression by immunostaining, 2.5×10^4 cells per 24 wells for real-time PCR, and 1.5×10^5 cells per 6-cm plate for analysis of HIV-1 infection by fluorescence-activated cell sorting [FACS], for Blam assay, and to control uptake of

FIG. 1. Characterization of the CD4-positive cell line HeLa4D9 stably expressing dyn^{ts} under the control of a tet-responsive promoter. (A) Fluorescence microscopy analysis of dyn^{ts} expression (left panel) and endocytosis of transferrin (right panel). HeLa4D9 cells were cultivated for 3 days at 32°C in the presence (c and c') or absence (a, a', b, and b') of tetracycline. Subsequently, cells were shifted to the nonpermissive temperature of 37°C for 1.5 h (a, a', c, and c') or were shifted to the permissive temperature of 30°C for 1 h after the 37°C treatment (b and b'). Twenty minutes before fixation, fluorescently labeled transferrin was added to determine inhibition of clathrin-dependent endocytosis. Cells were fixed and stained for the HA epitope tag on dyn^{ts} . Note that transferrin localization was slightly different when endocytosis assays were performed at 30°C, which is likely to be due to slower uptake kinetics at the lower temperature. (B) FACS analysis of surface expression of CD4 (left panels) and CXCR4 (right panels) on HeLa4D9 cells. Cells were cultivated for 3 days in the presence (heavy gray line) or absence (black line) of tetracycline and were subsequently shifted to the nonpermissive temperature of 37°C for 1.5 h (a and a') or were kept at the permissive temperature of 30°C (b and b'). Cells were fixed and stained with FITC-labeled antibody against CD4 (a and b) or PE-labeled antibody against CXCR4 (a' and b') and analyzed by flow cytometry. Negative controls (gray shading) are unstained cells or cells stained with a PE-labeled isotype control antiserum, respectively. The numbers indicate the percentage of positive cells.

transferrin) in the absence or presence of tet, respectively. After 48 h at 32°C, cells were incubated at 37°C for 1.5 to 2 h to establish the endocytosis-deficient phenotype or kept at 30°C. Virus was prewarmed to 37°C and added at the indicated multiplicity of infection (MOI). To avoid influences by tet on infection, cells were not exposed to tet during virus incubation. To control the efficiency of endocytosis inhibition, parallel cultures on coverslips were analyzed for transferrin uptake.

Virus production and titration. Stocks of HIV-1_{NL4-3}, HIV-1_{SF2}, and HIV-1_{MVP8161} were produced by cocultivation of infected and uninfected MT-4 cells (61). Uninfected cells (5×10^5 cells/ml) were mixed with infected cells at a ratio of 5:1 and virus was harvested before pronounced cytopathic effects were observed (24 to 36 h postinfection). Virus-containing supernatants were cleared by low-speed centrifugation, filtered through 0.45- μ m-pore-size filters (Schleicher & Schuell), and adjusted to 10 mM HEPES (pH 7.4). Aliquots were frozen at -80°C or in liquid nitrogen.

HIV-1 particles carrying the β -lactamase (Blam)-Vpr fusion protein were produced by cotransfection of 293T cells with the HIV-1 proviral plasmid pNL4-3 (6) and pMM310. HIV-1 particles pseudotyped with the VSV-G glycoprotein were produced by cotransfection of 293T cells with pNL4-3env⁻-GFP and pM3. Transfections were performed by using Lipofectamine 2000 (Invitrogen) according to the description of the manufacturer. After 48 h at 37°C, virus-containing culture media were harvested, cleared as described above, and concentrated 10-fold by centrifugation through an Amicon Ultra filter (30-kDa exclusion limit).

Virus titrations were performed in quadruplicate by using serial 10-fold dilutions of the respective virus. After incubation for 2 days at 37°C, HIV-1-infected cells were detected by staining with a monoclonal antibody to the CA protein and a secondary antibody conjugated with β -galactosidase (BIOZOL) as described previously (12).

Immunofluorescence and FACS analysis. The expression of dyn^{ts} was detected by using a FITC-conjugated monoclonal antibody to the epitope tag from influenza virus hemagglutinin (HA; Roche). Cells were fixed in 3.7% paraformaldehyde in phosphate-buffered saline (PBS) for 20 min at room temperature, followed by incubation in 50 mM ammonium chloride for 15 min and immunostaining. To analyze the inhibition of clathrin-dependent endocytosis by dominant-negative dynamin, cells were incubated with Alexa Fluor 568-labeled transferrin (Molecular Probes) 20 min prior to fixation as described above. Fluorescence was visualized on an IX70 epifluorescence microscope (Olympus), and images were captured and processed with Soft Imaging System and Adobe Photoshop.

For FACS analysis of HIV receptor expression, cells were fixed (Fix & Perm kit; Becton Dickinson), incubated with FITC-conjugated antibodies to CD4 and phycoerythrin (PE)-conjugated antibodies against CXCR4 (Becton Dickinson), respectively, and analyzed by using a FACScan (Becton Dickinson). FACS analysis of HIV-1-infected HeLa4D9 cells was performed 48 h after infection. Cells were fixed for 1 h at room temperature in 3.7% paraformaldehyde in PBS and stained for 30 min at room temperature in the dark with a monoclonal antibody to CA conjugated with PE (KCS7-RD1; Coulter) diluted 1:20 in 0.1% Triton X-100 in PBS containing 3% FCS.

Detection of virus entry using the β -lactamase assay. Cytosolic entry of HIV-1 particles carrying the Blam-Vpr fusion protein was analyzed as described previously (59). HeLa4D9 cells or transfected HeLa cells grown on coverslips were infected with HIV-1_{NL4-3} particles carrying the Blam-Vpr protein at the indicated MOI for 5 h. Fluorescently labeled transferrin (Molecular Probes) was added to transfected HeLa cells 20 min prior to washing. Cells were washed with CO₂-independent medium (Invitrogen) and loaded with the fluorescent Blam substrate CCF2/AM as described by the manufacturer (Pan Vera). Cells were incubated for 17 h at room temperature to allow cleavage of the substrate and subsequently washed and fixed with 3.7% paraformaldehyde in PBS. The relative number of cells fluorescent at 447 nm among GFP-expressing (detected after short bleaching of the uncleaved substrate at 520 nm) and GFP-negative cells was determined by microscopic analysis of at least 400 cells each.

Quantitation of RT products. To remove DNA from the virus preparation, HIV-1 particles were treated with 300 U of DNase (Roche)/ml for 30 min at 37°C. Cells were infected with DNase-treated virus and total DNA was isolated at different time points by using a QIAamp Blood Minikit (Qiagen) or DNazol (Invitrogen) according to the recommendations of the manufacturers. Quantification of RT products from the U3 region was performed by real-time PCR in the LightCycler (Roche) with the primers 48U3 (sense, TGGATCTACCACACAAGGCTA) and 118U3 (antisense, AGCACATCCAAAGGTCAGTG). Three independent analyses were performed for each sample, and serial dilutions of a pNL4-3 derivative in unspecific genomic DNA were used as a standard. For normalization, total DNA amounts of each sample were measured by pho-

tometry at 260 nm or the cellular single-copy gene encoding *gapdh* was quantified in parallel by real-time PCR.

RESULTS

Establishment of an HIV-infectible HeLa cell line expressing a dominant-negative variant of dynamin. To investigate the role of the endocytic pathway in the entry of HIV-1, we transduced a HeLa cell line containing a tightly regulated variant of dynamin (15) with a retrovirus vector carrying the human CD4 gene. The parental cells express a *trans* dominant-negative, temperature-sensitive mutant of dynamin (G273D; dyn^{ts}) (29) under control of a tetracycline-responsive promoter. In the absence of tet, expression of the dynamin mutant is induced, and efficient inhibition of clathrin-dependent endocytosis is observed at the nonpermissive temperature of 37 or 38°C (15). No inhibition occurs at the permissive temperature of 30°C. To score for inhibition, dyn^{ts} is first produced at the permissive temperature (30 to 32°C), allowing oligomerization with endogenous dynamin, and the temperature is then shifted to 37°C to induce the *trans*-dominant phenotype.

CD4-positive cells were initially isolated by magnetic separation of transduced cell populations and were shown to retain inducible expression of dyn^{ts} (data not shown). To establish a clonal cell line, single CD4-positive cells were isolated by FACS. Individual cell clones were analyzed for stable CD4 expression (Fig. 1B) and for inducible expression of dyn^{ts}, and the cell line HeLa4D9 was selected for further experiments. To test the inducible inhibition of clathrin-dependent endocytosis, HeLa4D9 cells were cultivated in the presence or absence of tet at 32°C for 3 days. Subsequently, cells were either shifted to the nonpermissive temperature for 1.5 h or were incubated for 1 h at 30°C after the 37°C shift. Twenty minutes before fixation, fluorescently labeled transferrin was added to monitor clathrin-mediated internalization. Expression of dyn^{ts} was analyzed with an antibody directed against the HA epitope tag on dyn^{ts}. No HA signal was detected when cells were repressed by cultivation in the presence of tet (Fig. 1Ac), and normal transferrin endocytosis was observed as indicated by the punctate staining in the perinuclear region (Fig. 1Ac'). Cultivation for 3 days in the absence of tet, on the other hand, yielded a strong signal for dyn^{ts} in HeLa4D9 cells, which was mainly observed in membrane ruffles and lamellipodia (Fig. 1Aa and b). When cells were kept at the permissive temperature, the uptake of fluorescently labeled transferrin was largely unaltered (Fig. 1Ab'), whereas clathrin-mediated endocytosis of transferrin was efficiently blocked after incubation at the nonpermissive temperature (Fig. 1Aa'). Weak staining at the plasma membrane, but no intracellular punctate staining, was observed in 80 to 95% of HeLa4D9 cells cultivated at 37°C. Thus, this cell line retains the inducible inhibition of clathrin-dependent endocytosis.

To determine whether inhibition of endocytosis interferes with the cell surface expression of the HIV-1 entry receptors, flow cytometric analyses were performed (Fig. 1B). Expression of dyn^{ts} was induced or suppressed in HeLa4D9 cells as described above, and cells cultivated for an additional 1.5 or 5 h at either 30 or 37°C were fixed and stained with antibodies against CD4 or CXCR4, respectively. As shown in Fig. 1B (left panel), there was no difference in CD4 surface expression and

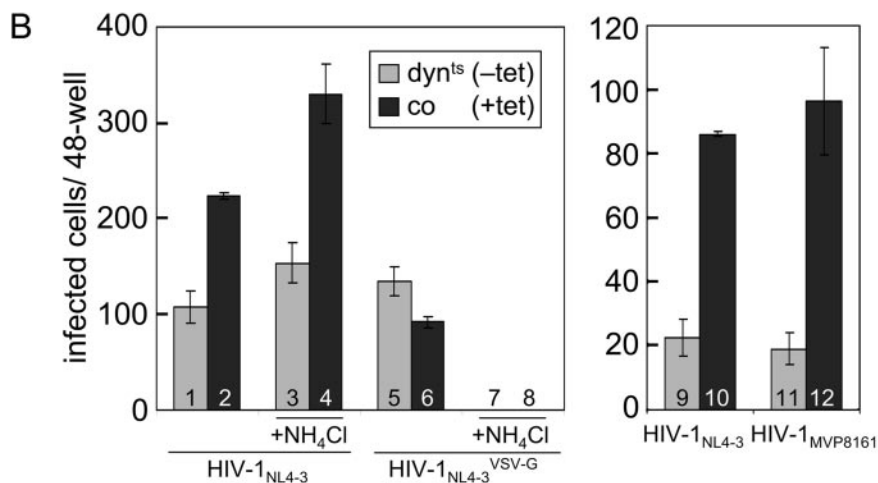
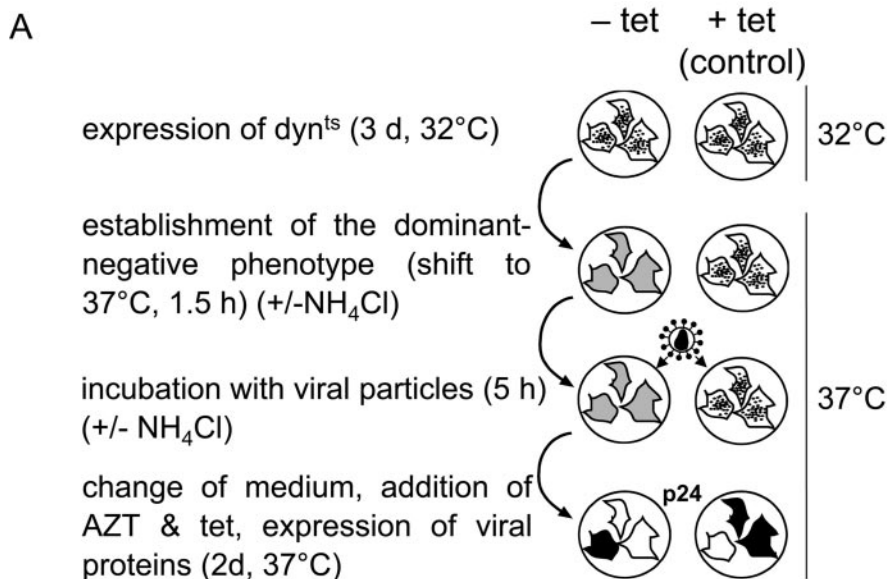


FIG. 2. Single round entry assay. (A) Schematic depiction of the entry assay. HeLa4D9 cells were cultivated for 3 days at 32°C in the absence (to induce dyn^{ts} expression) or presence of tetracycline. Subsequently, cells were shifted to the nonpermissive temperature of 37°C for 1.5 h, and 10 mM ammonium chloride (NH₄Cl) was added in some cases to study the influence of endosomal acidification. Cells were infected with HIV-1 particles or viral pseudotypes at the indicated MOIs and were further cultivated at 37°C for additional 4 to 7 h to allow HIV-1 entry. Subsequently, the medium was changed, azidothymidine was added at a concentration of 10 μM to prevent infection at later time points, and tetracycline was added to shut off dyn^{ts} expression. HIV-1 infection was evaluated after 2 days by staining with an antibody to the viral CA protein and detection with a secondary antibody conjugated to β-galactosidase (indicated as dark cells). The total number of CA-positive cells per well was counted. Punctate patterns on cells indicate normal endocytosis, gray areas indicate inhibition of endocytosis. (B) Representative single-round entry assays. HeLa4D9 cells were infected with HIV-1_{NL4-3} at an MOI of 0.06 with HIV-1_{NL4-3} pseudotyped with VSV-G or with the HIV-1 O-type isolate MVP8161. Ammonium chloride (NH₄Cl) was added 1.5 h prior to infection as indicated. The total numbers of HIV-1-infected cells are shown for HeLa4D9 cells cultivated in the absence (□) or presence (■) of tetracycline. Mean values of triplicate infections are shown, with error bars representing one standard deviation.

>98% of the cells were CD4 positive in every case, with a similar mean fluorescence intensity. The same result was observed for the HIV-1 coreceptor CXCR4 (Fig. 1B, right panel). CD4 and CXCR4 surface expression were also unchanged

after incubation for 5 h at 37°C (data not shown). Thus, HeLa4D9 cells represent a CD4-positive HeLa cell line that is suitable for the investigation of the influence of endocytosis on HIV-1 entry.

Dominant-negative dynamin leads to a strong reduction of HIV-1 infection in HeLa4D9 cells. To examine the influence of dynamin-dependent endocytosis on HIV-1 entry in a single-round infection assay, the following experimental protocol was established (Fig. 2A). The expression of dyn^{ts} was induced or suppressed in HeLa4D9 cells as described above, and cells were cultivated for an additional 1.5 h at 37°C to induce the dominant-negative phenotype. The effect of dyn^{ts} was confirmed by analyzing the internalization of transferrin in parallel samples (data not shown). Subsequently, HIV-1 particles were added at different MOIs, and incubation was continued for a further 5 to 7 h at 37°C. Medium was replaced, and tet was added to repress expression of dyn^{ts}. The half time of dyn^{ts} at 37°C was shown to be about 8 h, and no inhibition of endocytosis was observed 20 h after the readdition of tet (data not shown). Thus, a potential influence of residual dyn^{ts} on HIV-1 gene expression and virion formation could be excluded. Upon removal of the virus inoculum, the reverse transcriptase inhibitor azidothymidine was added to avoid subsequent infection by remaining particles. HIV-1 protein expression was detected after incubation for 2 days at 37°C by immunostaining for the HIV-1 CA protein.

Figure 2B shows the results of representative experiments. All assays were performed in 48 wells in triplicates, and mean values of the total number of infected cells are depicted. Infection of repressed HeLa4D9 cells cultivated in the presence of tet with HIV-1_{NL4-3} at an MOI of 0.06 yielded a mean number of 224 infected cells per well (Fig. 2B, bar 2). Infection of dyn^{ts}-expressing cells cultivated without tet, on the other hand, produced only 108 infected cells per well (Fig. 2B, bar 1), corresponding to a reduction by 52%. In an independent experiment, HIV-1_{NL4-3} infection in dyn^{ts}-expressing cells was reduced by 74% (Fig. 2B, bars 9 and 10). In total, more than 10 independent experiments were performed with an inhibitory range between 40 and 80% in dyn^{ts}-expressing cells. The results were similar when cells were shifted to 30°C after 5 h of virus infection, which led to an immediate reversal of the dominant-negative effect (data not shown). Furthermore, expression of dominant-negative dynamin also strongly reduced infection of HeLa4D9 cells with the isolates HIV-1_{SF2} (data not shown) and HIV-1_{MVP8161}, which belongs to the divergent group O of HIV-1. In the latter case, the number of infected cells was reduced by 85% (Fig. 2B, bars 11 and 12). There was no reduction in the number of infected cells, however, when dyn^{ts}-expressing HeLa4D9 cells were infected with HIV-1 particles lacking the viral glycoproteins and pseudotyped with the G glycoprotein of the pH-dependent VSV (VSV-G) (Fig. 2B, bars 5 and 6). This result was unexpected since VSV is known to enter target cells through the endosomal pathway (36).

To test whether acidification of the endosomal compartment plays a role in virus entry, the effect of ammonium chloride (NH₄Cl) on HIV-1 entry was analyzed. Infection of HeLa4D9 cells not expressing dyn^{ts} in the presence of 10 mM NH₄Cl led to an increase in the number of HIV-1-positive cells by ca. 50% (Fig. 2B, bars 2 and 4), a finding similar to previously published results (1, 21). A similar increase in infectivity was also observed when dyn^{ts}-expressing cells were infected in the presence of NH₄Cl, and the negative effect of dyn^{ts} on HIV-1 entry was maintained in this case (Fig. 2B, bars 3 and 4). HIV-1 particles pseudotyped with VSV-G were used as a control, and

infection with these particles was completely blocked by NH₄Cl (Fig. 2B, bars 7 and 8) as expected.

To analyze whether the inhibition of HIV-1 infection by dyn^{ts} is dependent on the MOI, the experimental protocol was adapted to FACS analysis. HeLa4D9 cells were suppressed or induced to express dyn^{ts}, infected with HIV-1_{NL4-3}, and stained for intracellular CA antigen 2 days after infection. Figure 3A shows the result of infection at an MOI of 0.08, again confirming a reduction of infectivity in dyn^{ts}-expressing cells by ca. 50%. Very similar results were obtained when infections were performed with an MOI of 0.24 or 0.72 (Fig. 3B). Taken together, these results indicate that a block in endocytosis strongly reduces HIV-1 entry in HeLa4D9 cells independent of the MOI, whereas endosomal acidification is not required.

The negative effect of dyn^{ts} on HIV-1 infection occurs prior to reverse transcription. To determine whether dyn^{ts} affects a step in early HIV-1 entry, the accumulation of RT products was examined in newly infected cells. A quantitative real-time DNA-amplification protocol was developed by detecting the U3 region of the HIV-1 genome, which is reverse transcribed at an intermediate stage of genome replication (Fig. 4A). To validate the protocol, HeLa cells lacking the CD4 receptor and HeLaP4 cells containing CD4 were infected in parallel with HIV-1_{NL4-3} at an MOI of 0.5. Total DNA was extracted at different times after infection and analyzed by real-time PCR (Fig. 4B). No U3 signal was observed immediately after infection (time zero). Subsequently, increasing amounts of RT products were detected in HeLaP4 cells, starting at 2 h postinfection (Fig. 4B). No RT products were detected in HeLa cells lacking CD4, indicating that endosomal uptake of HIV-1 in the absence of CD4, which has been shown to occur in HeLa cells (33), does not lead to reverse transcription (Fig. 4B).

To analyze the effect of dyn^{ts}-mediated inhibition of endocytosis on the generation of HIV-1 RT products, HeLa4D9 cells were induced or suppressed to express dyn^{ts} as described above, infected with HIV-1_{NL4-3} at an MOI of 0.29, and extracted at different time points after infection. Subsequently, U3 copy numbers were determined by real-time PCR and normalized for total DNA in the sample. Three independent PCRs were performed for each sample, and infections were done in triplicate (time zero) or quadruplicate (time 7 h). No U3 products were detected immediately after infection (Fig. 4C). After 7 h, ca. 240 copies of the U3 product per ng of DNA were detected in cells cultivated in the presence of tet. This number was reduced by 60% in cells that had been induced to express dyn^{ts}. Thus, the effect of dyn^{ts} on HIV-1 infection occurs at an early time point prior to the completion of reverse transcription.

Dominant-negative dynamin reduces cytosolic HIV-1 entry. To further define the step affected by dyn^{ts}, the cytosolic entry of HIV-1 cores was analyzed in HeLa4D9 cells by using the previously described β -lactamase (Blam) assay (59). This method involves infection of target cells with HIV-1 particles, carrying a fusion protein of Blam and the HIV-1 protein Vpr. Target cells are then loaded with a Blam substrate (CCF2/AM) that changes its fluorescence emission spectrum from green to blue after cleavage by the enzyme. Cleavage depends on receptor-mediated entry of HIV-1 releasing the Blam-Vpr fusion protein into the cytosol of the newly infected cell (9, 40) and can thus be used as a direct measure of viral entry. To analyze

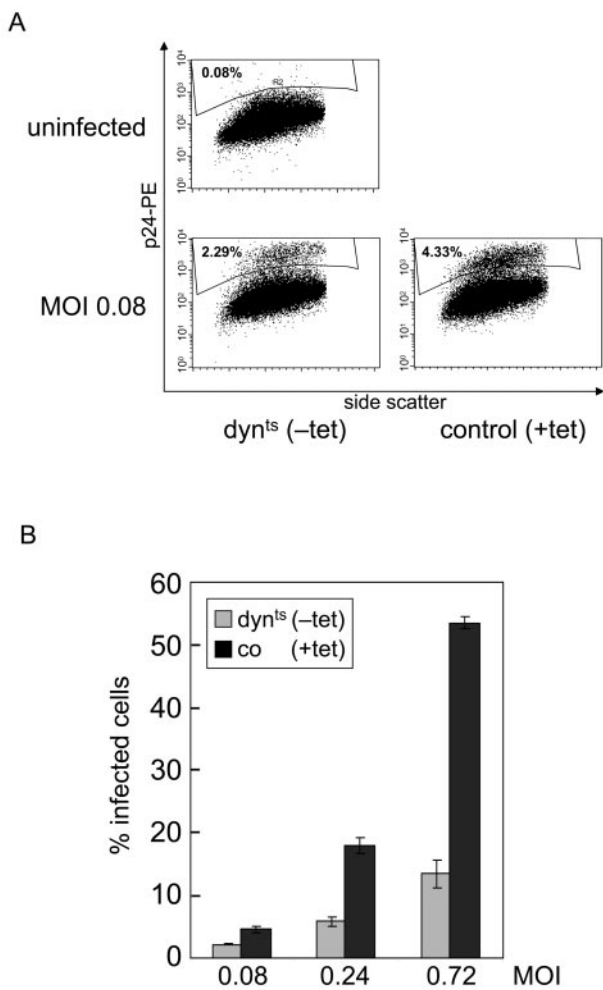


FIG. 3. Single round entry assays at different MOI. (A) Single-round entry assay on HeLa4D9 cells infected with HIV-1_{NL4-3} at an MOI of 0.08 as described in Fig. 2A. At 2 days after infection, cells were stained for intracellular CA antigen with a PE-conjugated monoclonal antibody and were analyzed by flow cytometry. Dot plots depict side scatter and fluorescence intensities for cells cultivated in the absence (left panels) or presence (right panel) of tetracycline. The percentage of infected cells is indicated. (B) HeLa4D9 cells were infected with HIV-1_{NL4-3} at MOIs of 0.08, 0.24, and 0.72 and analyzed by FACS as described above. Percentages of HIV-1-infected cells are shown for HeLa4D9 cells cultivated in the absence (□) or presence (■) of tetracycline as described in Fig. 2A. The mean values of triplicate infections are shown, with error bars representing one standard deviation.

the effect of dyn^{ts}-mediated inhibition of endocytosis on cytosolic entry of HIV-1, HeLa4D9 cells were induced or suppressed to express dyn^{ts} as before and infected for 5 h with HIV-1_{NL4-3} particles carrying the Blam-Vpr fusion protein at MOIs of 0.074 and 0.185, respectively. Cells were subsequently loaded with the Blam substrate, and the accumulation of the blue fluorescent product was analyzed by fluorescence microscopy. Uptake of the Blam substrate was detected in the green channel (Fig. 5Aa' and b'), whereas the cleaved product was observed in the blue channel (Fig. 5Aa and b). HIV-1 entry led to a strong blue fluorescence (Fig. 5A, arrows). The number of blue fluorescent cells was significantly reduced in HeLa4D9

cells expressing dyn^{ts} compared to control cells (Fig. 5A, compare panels a and b, and B).

Figure 5B shows a quantitative analysis of HIV-1 entry in HeLa4D9 cells induced or repressed for dyn^{ts} expression. Approximately 50% of control cells but only 20% of cells expressing dyn^{ts} exhibited blue fluorescence at an MOI of 0.185, a finding corresponding to a reduction in cytosolic HIV-1 entry by 60% (Fig. 5B). A similar reduction in HIV-1 entry was observed at an MOI of 0.074 (28% versus 11%; Fig. 5B). One should also note that the percentage of blue cells is significantly higher than the respective MOI. Virus titers had been determined on HeLa4D9 cells by analysis of CA expression, and the differences indicate that cytosolic entry may not necessarily lead to productive infection.

Blocking endocytosis in transiently transfected cells also reduces HIV-1 entry. The described results showed that the dominant-negative dynamin variant G273D strongly reduces entry of various HIV-1 isolates in the HeLa4D9 cell line. To determine whether this effect is dependent on the specific cell line and mutant, we performed infection experiments on transiently transfected HeLaP4 cells. Cells were transfected with expression constructs for fusion proteins of GFP with either wild-type (wt) dynamin or mutant dyn^{K44A}. This mutant also has a *trans* dominant-negative effect on the release of endocytic vesicles from the plasma membrane but differs from dyn^{G273D} in the ability to affect actin at the plasma membrane and is not temperature sensitive (42). At 42 h after transient transfection, cells were infected with HIV-1_{NL4-3} particles carrying the Blam-Vpr protein at an MOI of 0.2 for 4 to 5 h at 37°C. At 20 min before the end of the infection period, fluorescently labeled transferrin was added to monitor the inhibition of endocytosis. Subsequently, cells were loaded with the Blam substrate as described above and investigated under the fluorescence microscope. The upper two panels in Fig. 6 show the results for cells transfected with dyn^{K44A}GFP (Fig. 6a) and dyn^{wt}GFP (Fig. 6b). Detection of the respective GFP fusion protein in the green channel was partly obscured by the uncleaved Blam substrate and was only possible after rapid bleaching of this substrate (Fig. 6a'' and b''). Thus, only cells showing a strong expression of the GFP fusion protein were identified as productively transfected cells and are marked in Fig. 6. Cells transfected with dyn^{K44A}GFP generally exhibited a strong block in transferrin endocytosis (Fig. 6a and a'', arrows), whereas cells transfected with dyn^{wt}GFP revealed normal transferrin uptake (Fig. 6b and b'', arrowheads) as expected. HIV-1 entry was analyzed in the blue channel, revealing virtually no blue fluorescent cells among the strongly GFP-positive population in the case of dyn^{K44A}GFP transfection (Fig. 6a', arrows), whereas blue fluorescent cells were readily detected in the GFP-positive population of dyn^{wt}GFP transfection (Fig. 6b', arrowheads). Importantly, relative HIV-1 entry as measured by blue fluorescence in neighboring cells not expressing detectable amounts of the respective dynamin variant was similar in both cultures (Fig. 7A, black bars), indicating that the entry block was due to expression of the dominant-negative dynamin variant.

Quantitative determination of HIV-1 entry was performed for three different cell populations in the case of dyn^{K44A}GFP as follows: (i) GFP-negative cells not expressing the respective dynamin variant (Fig. 7, solid bars), (ii) GFP-positive cells not

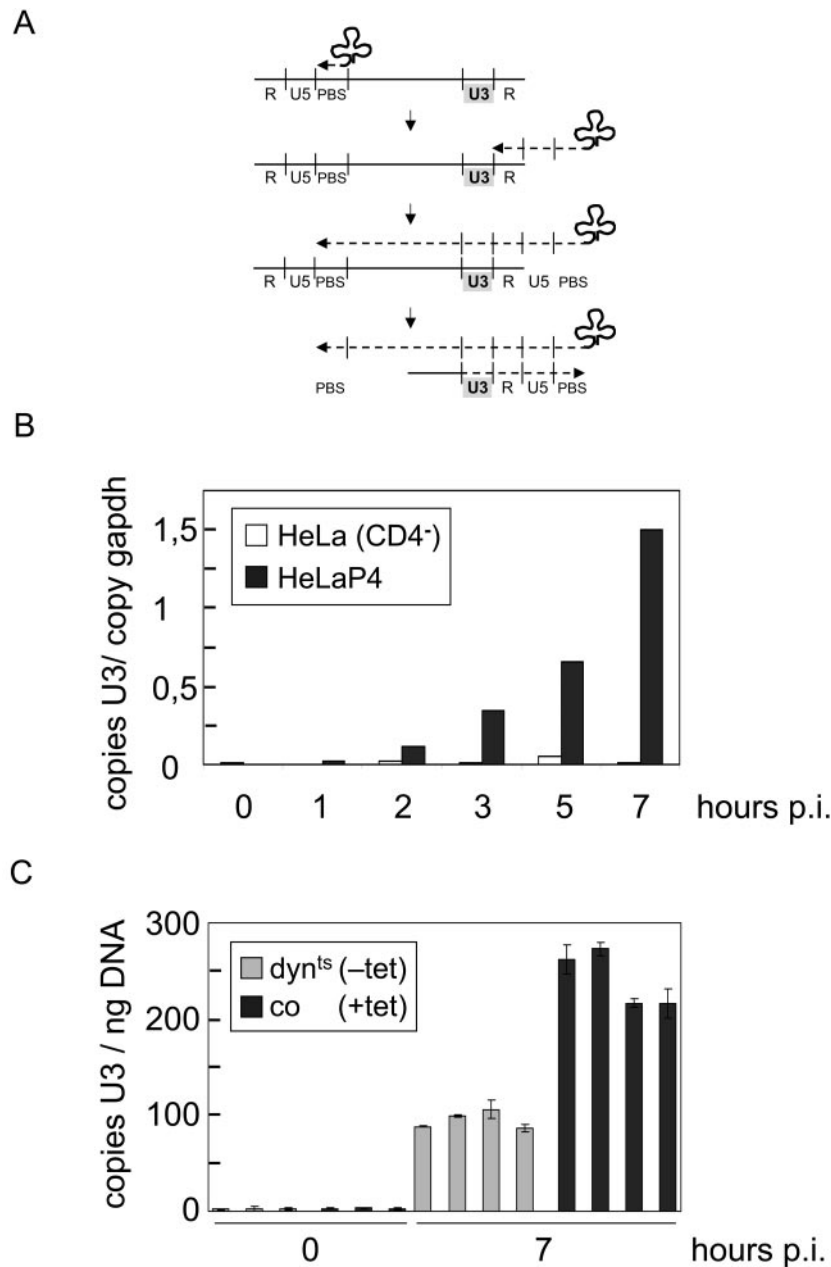


FIG. 4. Analysis of RT products in HIV-1 entry. (A) Schematic depiction of HIV-1 RT. Primer tRNA annealed to the primer binding site of the genomic RNA is extended to the 5' end, and strong-stop DNA is subsequently transferred to the 3' end of the genome, where it is elongated. RNA is shown as a bold line; DNA is shown as a dotted line. The U3 region amplified by the PCR primers is shaded gray. (B) Kinetic analysis of HIV-1 reverse transcription. HeLaP4 cells (■) or HeLa cells lacking the CD4 receptor (□) were infected with HIV-1_{NL4-3} at an MOI of 0.5. Total cellular DNA was extracted at the indicated time points and analyzed by real-time PCR. The copy number was determined by parallel analysis of a plasmid standard, and the results were normalized for copies of the *gapdh* gene. Means of duplicate infections are shown. (C) Quantitative analysis of HIV-1 reverse transcription products in cells expressing or lacking dyn^{ts}. HeLa4D9 cells were infected with DNase-treated HIV-1_{NL4-3} at an MOI of 0.29 as described in Fig. 2A. Total cellular DNA was extracted immediately after infection or after 7 h at 37°C and analyzed by real-time PCR as described above. U3 copy numbers (normalized for total DNA) are shown for HeLa4D9 cells cultivated in the absence (□) or presence (■) of tetracycline. Mean values of three independent PCR analyses for triplicate (0 h) or quadruplicate (7 h) infections are shown, with error bars representing one standard deviation. p.i., postinfection.

inhibited in transferrin uptake (i.e., functionally wild-type; Fig. 7A, open bars), and (iii) GFP-positive cells blocked in endocytosis (e.g., arrows in Fig. 6a; Fig. 7A, shaded bars). In the case of dyn^{wt}GFP transfection, HIV-1 entry was determined for GFP-positive and GFP-negative cells (Fig. 7A). Evaluation

of at least 400 cells per population in triplicate samples revealed blue fluorescence in 50 to 60% of the GFP-negative population in both transfections after infection at an MOI of 0.2 (Fig. 7A, black bars). HIV-1 entry was reduced 10-fold in HeLa cells productively transfected with dyn^{K44A}GFP and

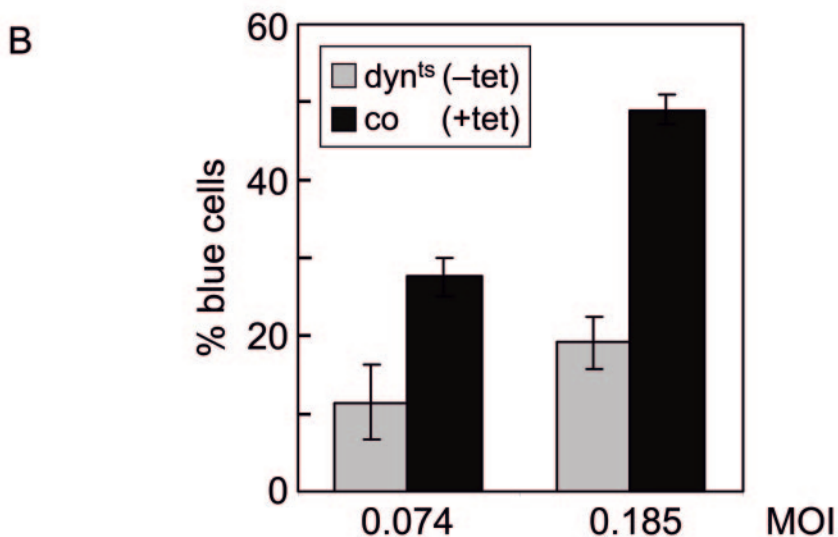
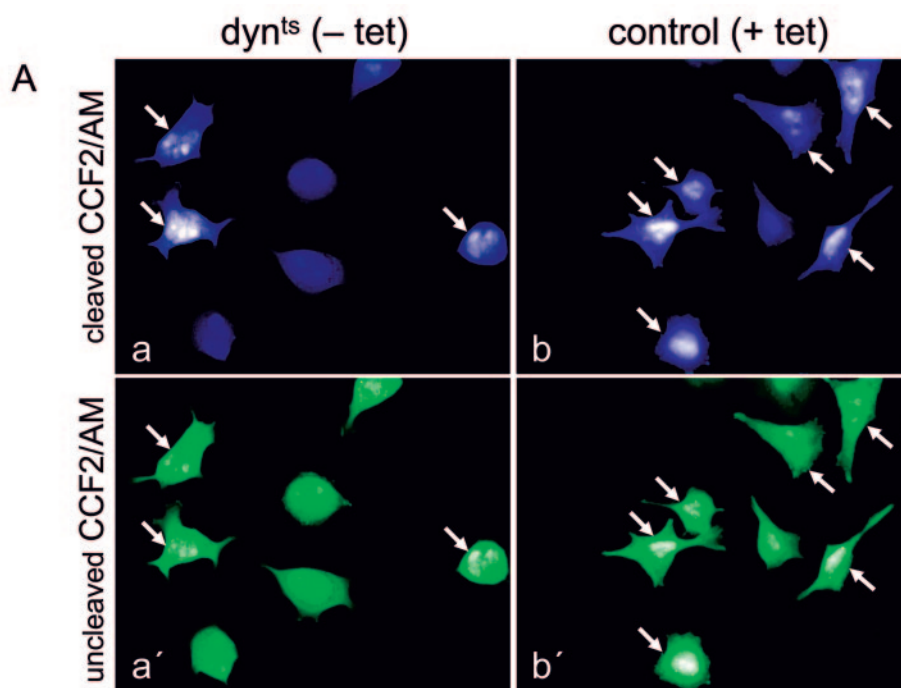


FIG. 5. Analysis of HIV-1 entry using the β -lactamase (Blam) assay. (A) HeLa4D9 cells cultivated in the absence (a and a') or presence (b and b') of tetracycline were infected with HIV-1 particles carrying the Blam-Vpr fusion protein at an MOI of 0.185 as described in Fig. 2A. After 5 h at 37°C, cells were loaded with the green fluorescent Blam substrate CCF2/AM. Cells were analyzed for the blue fluorescent cleavage product by fluorescence microscopy at a wavelength of 447 nm (a and b) and for the green fluorescent substrate at a wavelength of 520 nm (a' and b') (9, 59). Infected cells were strongly fluorescent in the blue channel (arrows). Note that uninfected cells exhibited a weak blue fluorescence in the blue channel as a result of false coloration. This was due to detection of the green fluorescent substrate in the blue channel but could be clearly distinguished from the blue signal of the cleavage product in the microscope. (B) HeLa4D9 cells cultivated in the absence (□) and presence (■) of tetracycline were infected with HIV-1 particles carrying the Blam-Vpr fusion protein at MOIs of 0.074 and 0.185. Blam activity was determined by fluorescence microscopy as described above. Mean values of triplicate infections (400 to 800 cells per infection analyzed) are shown, with error bars representing one standard deviation. Background levels determined as relative numbers of blue fluorescent cells in uninfected HeLa4D9 cells were subtracted ($6.8 \pm 0.8\%$ for cells cultivated in the absence and $0.5\% \pm 0.17\%$ for cells cultivated in the presence of tetracycline).

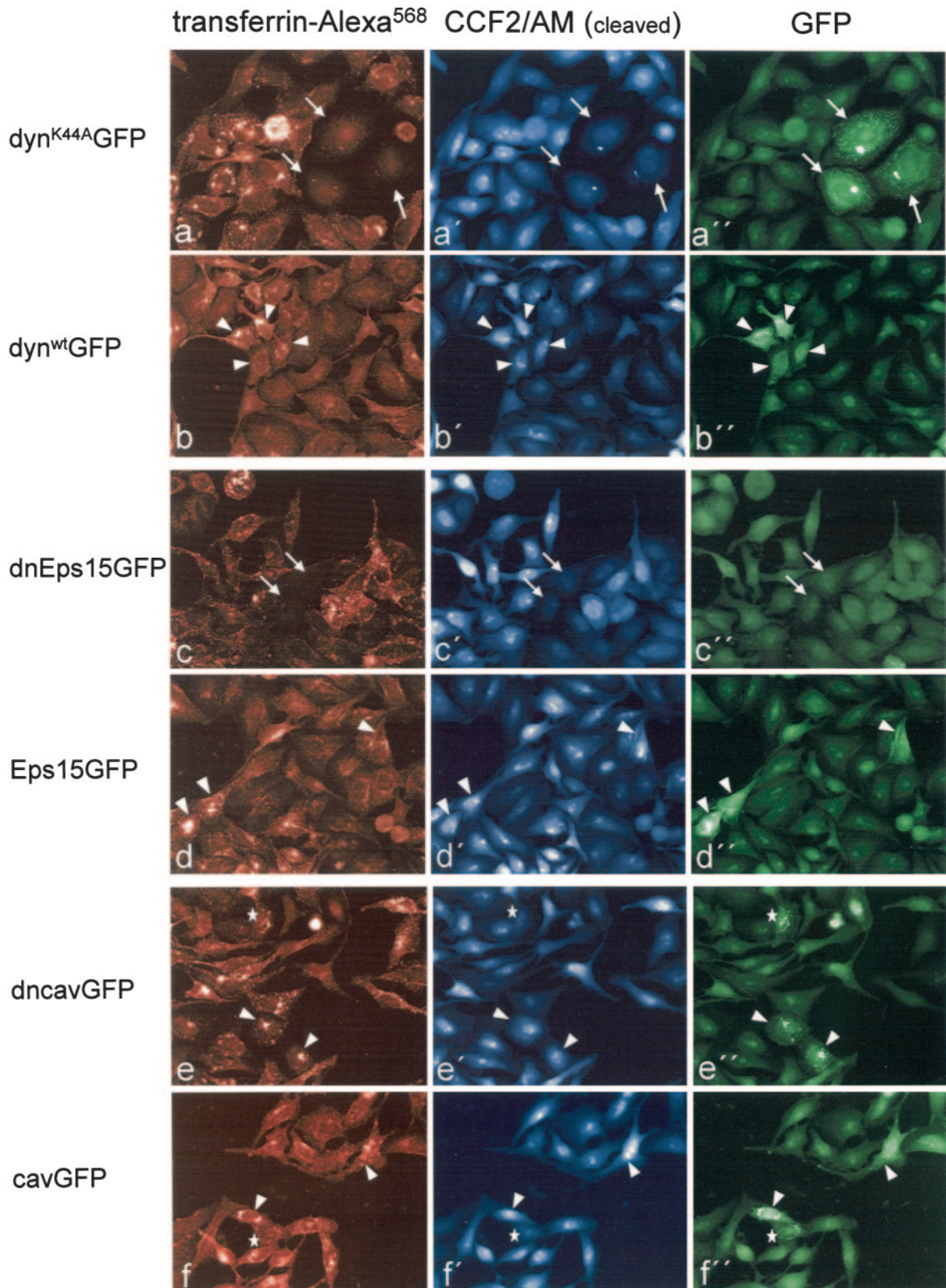


FIG. 6. Analysis of HIV-1 entry in transiently transfected HeLaP4 cells. HeLaP4 cells were transfected with the indicated expression constructs. At 42 h after transfection, cells were infected with HIV-1 particles carrying Blam-Vpr at an MOI of 0.2. Cells were incubated for 5 h at 37°C, and fluorescently labeled transferrin was added 20 min before cells were loaded with the Blam substrate CCF2/AM. Cells were analyzed for endocytosis

blocked in endocytosis (Fig. 7A, gray bar). Little inhibition was observed in dyn^{K44A} GFP-transfected cells that were not blocked in endocytosis and in cells transfected with dyn^{WT} GFP (Fig. 7A, open bars). Thus, blocking endocytosis by expression of the dyn^{K44A} variant in HeLaP4 cells strongly reduced HIV-1 entry, confirming the results obtained for the HeLa4D9 cell line.

HIV-1 entry is inhibited by expression of dominant-negative Eps15 but not by expression of dominant-negative caveolin.

Dynamain plays a role in several endocytic pathways and the observed effect of dominant-negative dynamain expression does not directly identify the pathway important for HIV-1 entry. To further delineate the molecular mechanism of entry inhibition, we performed experiments with *trans* dominant-negative versions of Eps15 and caveolin, respectively. Dominant-negative Eps15 specifically affects the internalization of clathrin-coated vesicles by interacting with AP2 (3), whereas caveolin-1 fused to GFP at its N terminus (dncavGFP) has been shown to inhibit the entry of the caveola-dependent SV40. In contrast, C-terminal fusion to GFP (cavGFP) did not interfere with the entry of SV40 (49).

HeLaP4 cells were transiently transfected with constructs expressing GFP fused with wild-type or dominant-negative Eps15 and with wild-type or dominant-negative caveolin-1. At 42 h after transient transfection, cells were infected with HIV-1_{NL4-3}, carrying the Blam-Vpr protein at an MOI of 0.2 for 4 to 5 h at 37°C. Fluorescently labeled transferrin was added to monitor the inhibition of endocytosis, and cells were loaded with the Blam substrate as described above. The lower four panels in Fig. 6 show the results for cells transfected with dnEps15GFP (Fig. 6c), Eps15GFP (wild-type, Fig. 6d), dncavGFP (Fig. 6e), and cavGFP (Fig. 6f). Expression of the respective GFP fusion protein was analyzed in the green channel after rapid bleaching of the uncleaved Blam substrate as described above. This was clearly detectable in the case of the caveolin-1 GFP fusion proteins (Fig. 6e' and f', arrowheads) and of wild-type Eps15GFP (Fig. 6d'), whereas no GFP signal was detectable in the case of the dnEps15 fusion due to low expression levels (Fig. 6c'). Cells expressing dnEps15GFP were therefore identified by their strong block in transferrin endocytosis (Fig. 6c, arrows). HIV-1 entry was analyzed in the blue channel, revealing a strong reduction in the number of blue fluorescent cells when dnEps15GFP-transfected cells that were blocked in transferrin endocytosis (Fig. 6c, arrows) were compared to neighboring cells exhibiting normal transferrin endocytosis. Quantitative analysis of more than 400 cells revealed a 20-fold decrease in HIV-1 entry from ca. 60% in the case of cells with normal transferrin endocytosis to ca. 3% in the case of cells blocked in transferrin endocytosis (Fig. 7B, left panel). In contrast, there was no significant difference in the number of blue fluorescent cells when the strongly GFP-positive and -negative populations were compared after transfection

of wild-type Eps15GFP (Fig. 6d and 7B, right panel). Analysis of cells transfected with dominant-negative dncavGFP or wild-type cavGFP also revealed no significant difference in the relative entry of HIV-1. Similar numbers of blue cells were observed in the GFP-positive and GFP-negative cell populations in both cases (Fig. 6e and f and 7C), indicating that caveolae do not play a role in HIV-1 entry.

DISCUSSION

In this report, the role of endocytosis for productive entry of HIV-1 was investigated by using *trans* dominant-negative proteins that interfere with specific endocytic routes. Inhibition of dynamain in a stable inducible cell line, as well as upon transient expression, led to a marked reduction (40 to 90%) of the number of cells productively infected with HIV-1. This reduction was independent of the MOI used and was observed for two subtype B isolates and one O group isolate of HIV-1. Inhibition occurred at the stage of entry and was detected by quantification of RT products and of delivery of HIV-1 cores into the cytosol. Comparable effects were obtained upon inhibition of clathrin-mediated endocytosis by a dominant-negative mutant of Eps15, whereas a caveolin-1 mutant that inhibits caveola-dependent entry of SV40 (48) had no significant effect. Together, these results demonstrate that HIV-1 can productively infect cells via an endocytic route that involves clathrin-coated vesicles and is regulated by dynamain. It is also noteworthy that direct measurement of cytosolic entry of HIV-1 by using the Vpr-Blam fusion protein yielded a three- to fourfold higher number of infected cells than did the determination of viral structural protein expression after 48 h. If we assume comparable sensitivities of both assays, one may conclude that a large number of HIV cores that successfully gained access to the host cell cytoplasm failed to initiate a productive infection. This is likely to reflect the activity of cellular restriction factors, such as Ref1 (reviewed in reference 5).

Endocytosis of HIV-1 particles by clathrin-coated vesicles has been observed in previous studies with electron (23, 24, 45) and fluorescence (33) microscopy but has generally been considered a dead-end pathway. This conclusion is largely based on the observation that HIV-1 infectivity was increased rather than decreased by blocking endosomal acidification by using, e.g., ammonium chloride or bafilomycin A (1, 21, 33). Furthermore, Maréchal et al. (33) reported that endosomal uptake of HIV-1 occurs independently of cellular receptor and viral glycoprotein, whereas cytosolic accumulation of viral antigen is strictly dependent on these factors. Although these reports provided clear evidence that there is no pH-dependent step in HIV-1 entry, they do not argue against pH-independent endosomal entry, as has been reported for poliovirus (16, 50). Indeed, it is difficult to explain why there should be no productive HIV-1 fusion from early endosomes (prior to acidification) if

of labeled transferrin (left panels, a to f), for HIV-1 infection as indicated by the blue fluorescent Blam cleavage product (middle panels, a' to f'), and for productive transfection as indicated by GFP detection (right panels, a'' to f''). Note that uncleaved CCF2/AM was also detected in the GFP channel and obscured weak GFP signals. Accordingly, only strongly GFP-positive cells could be scored and dnEps15GFP, which yielded a very weak signal, could not be detected by fluorescence analysis. Block of transferrin endocytosis was used to identify productively transfected cells in this case. Arrows identify cells with inhibited transferrin uptake (see left panel), arrowheads identify GFP-positive cells infected with HIV-1, and asterisks identify GFP-positive cells not infected with HIV-1. A representative experiment is shown. All signals are shown as false colors.

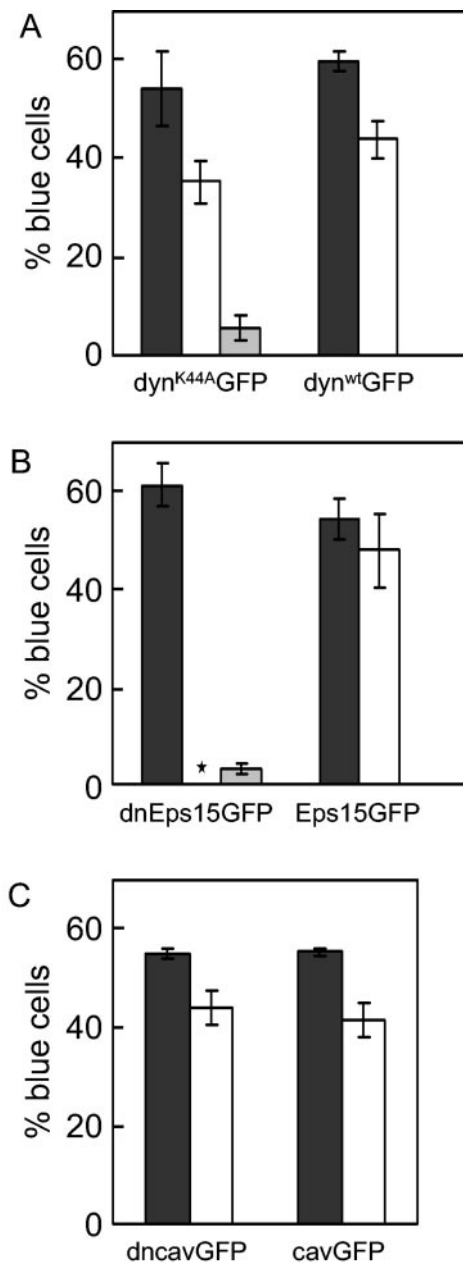


FIG. 7. Quantitative analysis of HIV-1 cytosolic entry. HeLaP4 cells were transiently transfected with constructs expressing GFP fusion proteins with wild-type or mutant dynamin (A), wild-type or mutant Eps15 (B), or wild-type or mutant caveolin (C). At 42 h after transfection, cells were infected with HIV-1 particles carrying the Blam-Vpr fusion protein at an MOI of 0.2. Cells were incubated and treated as described in the legend to Fig. 6. HIV-1 infection (as indicated by the blue fluorescent Blam product) of cells was scored in three groups according to expression of the GFP fusion protein and to inhibition of endocytosis. Nontransfected cells (GFP negative) (■), productively transfected cells exhibiting normal transferrin endocytosis (GFP positive, punctate pattern of fluorescently labeled transferrin) (□), and productively transfected cells with blocked endocytosis (GFP positive, transferrin negative) (▣) are indicated. For dnEps15 in panel B, only transferrin internalizing (■) and transferrin-negative (▣) cells were scored due to the weak GFP fluorescence (compare with Fig. 6). The mean values of three independent infections (five independent infections in case of dnEps15GFP, Eps15GFP, and *dyn^{K44A}GFP*) are shown with >400 cells analyzed in total per population. The error bars represent one standard deviation. Background blue fluorescence in uninfected cells was observed in <1% of cells.

receptor and coreceptor are present in the respective vesicle. Productive endosomal entry of HIV-1 has been suggested in several recent studies at least for certain cell types and virus strains (19, 34, 52). We show here that endosomal entry contributes significantly to productive HIV-1 entry in HeLa cells.

Our confidence in this statement is based on multiple aspects of the study. We examined the role of endocytic pathways by inhibiting vesicle release from the plasma membrane with well-characterized dominant-negative proteins, avoiding side effects on other cellular functions by chemicals. HIV-1 entry was significantly reduced in the *dyn^{ts}* cell line (40 to 80%), as well as upon transient expression of the *dyn^{K44A}* mutant (90%). No entry inhibition was observed in the inducible *dyn^{ts}* cell line at the permissive temperature, which allowed us to exclude that nonspecific interference by *dyn^{ts}*—independent of its role in endocytosis—caused the effect. This was also confirmed by the direct correlation between transferrin uptake and HIV-1 entry in the experiments with *dyn^{K44A}GFP*. Importantly, the effects of dynamin inhibition on HIV-1 infection were not due to changes in the cell surface levels of CD4 and CXCR4 molecules. The slightly lower inhibition by *dyn^{ts}* compared to *dyn^{K44A}* was likely due to an incomplete inhibition of endocytosis in the *dyn^{ts}*-expressing cell population (5 to 20% of HeLa4D9 cells were still internalized transferrin upon induction of *dyn^{ts}*). Inhibition of HIV-1 entry upon interference with dynamin function was observed by several independent experimental approaches analyzing selected steps of the entry process. Of note, the effect was independent of the MOI and virus isolate, excluding artifacts due to overloading the cells with HIV-1 particles. We therefore conclude that dynamin and Eps15 are critical for an endocytic entry pathway that is used by multiple HIV-1 isolates. In contrast, we did not find evidence for an involvement of caveolae in HIV-1 entry, which is in line with the fact that T cells, the natural target of HIV-1, do not express caveolin (20).

Since HIV-1 particles are efficiently taken up by clathrin-coated vesicles (23, 24, 33) and given the critical role of dynamin in the release of these vesicles from the plasma membrane, our data are best compatible with a model wherein endocytic entry of HIV-1 occurs via receptor- and coreceptor-mediated release of virions from endosomal vesicles. We cannot exclude, however, that inhibition of endocytosis may affect recycling of another, as yet unknown, entry cofactor different from CD4 and coreceptor. Clearly, endocytic entry does not require endosomal acidification as was confirmed in the present study by using ammonium chloride treatment. Accordingly, productive entry of HIV-1 may occur in endosomal compartments prior to acidification, whereas the majority of endosomal HIV-1 particles is destroyed by the low pH in the late endosome and/or lysosome, with only 10 to 40% of intracellular HIV antigen reaching the cytosol (33). If acidification is blocked, endosomal virions may retain their infectivity for extended periods of time, which could explain the increased rate of infection. Interestingly, however, infectivity enhancement by ammonium chloride was also observed if endosomal entry was arrested by dominant-negative dynamin, where no endosomal acidification is expected to occur. This could be due to local pH alterations in plasma membrane-proximal vesicles or to ammonium chloride-induced changes in cell surface structures supporting HIV binding and/or fusion.

Although HIV-1 entry was significantly impaired by dominant-negative dynamin, there was little effect on HIV particles pseudotyped with the VSV-G glycoprotein. This result was unexpected given that VSV is a classical example of a virus entering the cell via a pH-sensitive endocytic route. Moreover, infection of HIV-1 particles pseudotyped with VSV-G was efficiently blocked by ammonium chloride, thus confirming its pH-dependent entry. Thus, HIV-1/VSV-G pseudotypes appear to infect HeLa cells via a dynamin-independent, pH-dependent route. The infectivity of VSV-G pseudotyped murine leukemia virus, on the other hand, was strongly reduced in target cells expressing dyn^{K44A} (31), whereas wild-type murine leukemia virus entered the cells in a dynamin-independent manner. It is currently not clear why pseudotyping retroviral particles with VSV-G should have variable effects on the nature of the entry route. Alternatively, different dynamin mutants might have different effects, and this warrants further investigation.

Inhibition of HIV-1 entry by dominant-negative dynamin and Eps15 varied between ca. 40 and 95% depending on the experimental conditions. The remaining infectivity is likely to be due to direct virus entry at the plasma membrane, which would be in line with previous reports showing that HIV-1 infection does not require endocytosis. Choosing the endocytic route may have advantages for the virus, however. Fusion at the plasma membrane brings the entering particle to the subcortical actin cytoskeleton, which constitutes a difficult barrier to overcome. Fusion from endosomal particles, on the other hand, delivers the HIV-1 core directly into the cytosol, where replication may be pursued, provided the virus can escape the endosome before it is inactivated by low pH. One may predict, therefore, that the relative contribution of HIV-1 fusion at the plasma membrane and within endosomal vesicles depends on the relative thickness of the submembrane cytoskeleton, the rate of endosomal uptake, the kinetics of endosomal acidification, and the fusion kinetics of the respective virus and cell. The present study provides evidence for a significant contribution of clathrin-dependent endocytosis on HIV-1 entry in HeLa cells, which may be surprisingly efficient given the 10- to 20-fold inhibition by dominant-negative mutants in transiently transfected cells. It appears likely that this entry route is also utilized in other target cells, whereas the efficiency and the exact pathway of internalization may vary. Future studies will investigate the relevance of endocytic entry in T-cell lines and in physiological HIV-1 target cells such as primary T cells and macrophages. Based on our results, one may predict, however, that pH-independent endosomal entry is a more common phenomenon in virus entry that may not have been detected because of the study systems applied.

ACKNOWLEDGMENTS

We thank S. Schmid for the parental dyn^{ts} cells and B. Schwappach for sorting the transduced dyn^{ts} cells. We are grateful to A. Dautry-Varsat, A. Helenius, P. Clapham, D. Gabuzda, N. Landau, and D. von Laer for gifts of plasmids and cells and to T. Giese for help with real-time PCR and for the GAPDH gene specific primers. We thank O. Keppler for help with FACS analysis of infected HeLa4D9 cells.

REFERENCES

- Aiken, C. 1997. Pseudotyping human immunodeficiency virus type 1 (HIV-1) by the glycoprotein of vesicular stomatitis virus targets HIV-1 entry to an endocytic pathway and suppresses both the requirement for Nef and the sensitivity to cyclosporin A. *J. Virol.* **71**:5871–5877.
- Andersen, K. B., and B. A. Nexø. 1983. Entry of murine retrovirus into mouse fibroblasts. *Virology* **125**:85–98.
- Benmerah, A., M. Bayrou, N. Cerf-Bensussan, and A. Dautry-Varsat. 1999. Inhibition of clathrin-coated pit assembly by an Eps15 mutant. *J. Cell Sci.* **112**(Pt. 9):1303–1311.
- Benmerah, A., C. Lamaze, B. Begue, S. L. Schmid, A. Dautry-Varsat, and N. Cerf-Bensussan. 1998. AP-2/Eps15 interaction is required for receptor-mediated endocytosis. *J. Cell Biol.* **140**:1055–1062.
- Bieniasz, P. D. 2003. Restriction factors: a defense against retroviral infection. *Trends Microbiol.* **11**:286–291.
- Bohne, J., and H. G. Krausslich. 2004. Mutation of the major 5' splice site renders a CMV-driven HIV-1 proviral clone Tat-dependent: connections between transcription and splicing. *FEBS Lett.* **563**:113–118.
- Brandt, S. M., R. Mariani, A. U. Holland, T. J. Hope, and N. R. Landau. 2002. Association of chemokine-mediated block to HIV entry with coreceptor internalization. *J. Biol. Chem.* **277**:17291–17299.
- Cao, H., F. Garcia, and M. A. McNiven. 1998. Differential distribution of dynamin isoforms in mammalian cells. *Mol. Biol. Cell* **9**:2595–2609.
- Cavrois, M., C. De Noronha, and W. C. Greene. 2002. A sensitive and specific enzyme-based assay detecting HIV-1 virion fusion in primary T lymphocytes. *Nat. Biotechnol.* **20**:1151–1154.
- Charneau, P., M. Alizon, and F. Clavel. 1992. A second origin of DNA plus-strand synthesis is required for optimal human immunodeficiency virus replication. *J. Virol.* **66**:2814–2820.
- Chesebro, B., R. Buller, J. Portis, and K. Wehrly. 1990. Failure of human immunodeficiency virus entry and infection in CD4-positive human brain and skin cells. *J. Virol.* **64**:215–221.
- Clapham, P. R., A. McKnight, and R. A. Weiss. 1992. Human immunodeficiency virus type 2 infection and fusion of CD4-negative human cell lines: induction and enhancement by soluble CD4. *J. Virol.* **66**:3531–3537.
- Damke, H., T. Baba, A. M. van der Blik, and S. L. Schmid. 1995. Clathrin-independent pinocytosis is induced in cells overexpressing a temperature-sensitive mutant of dynamin. *J. Cell Biol.* **131**:69–80.
- Damke, H., T. Baba, D. E. Warnock, and S. L. Schmid. 1994. Induction of mutant dynamin specifically blocks endocytic coated vesicle formation. *J. Cell Biol.* **127**:915–934.
- Damke, H., M. Gossen, S. Freundlieb, H. Bujard, and S. L. Schmid. 1995. Tightly regulated and inducible expression of dominant interfering dynamin mutant in stably transformed HeLa cells. *Methods Enzymol.* **257**:209–220.
- DeTulleo, L., and T. Kirchhausen. 1998. The clathrin endocytic pathway in viral infection. *EMBO J.* **17**:4585–4593.
- Dimitrov, A. S., X. Xiao, D. S. Dimitrov, and R. Blumenthal. 2001. Early intermediates in HIV-1 envelope glycoprotein-mediated fusion triggered by CD4 and coreceptor complexes. *J. Biol. Chem.* **276**:30335–30341.
- Doms, R. W., and D. Trono. 2000. The plasma membrane as a combat zone in the HIV battlefield. *Genes Dev.* **14**:2677–2688.
- Fackler, O. T., and B. M. Peterlin. 2000. Endocytic entry of HIV-1. *Curr. Biol.* **10**:1005–1008.
- Fra, A. M., E. Williamson, K. Simons, and R. G. Parton. 1995. De novo formation of caveolae in lymphocytes by expression of VIP21-caveolin. *Proc. Natl. Acad. Sci. USA* **92**:8655–8659.
- Fredericksen, B. L., B. L. Wei, J. Yao, T. Luo, and J. V. Garcia. 2002. Inhibition of endosomal/lysosomal degradation increases the infectivity of human immunodeficiency virus. *J. Virol.* **76**:11440–11446.
- Gold, E. S., D. M. Underhill, N. S. Morrisette, J. Guo, M. A. McNiven, and A. Aderem. 1999. Dynamin 2 is required for phagocytosis in macrophages. *J. Exp. Med.* **190**:1849–1856.
- Goto, T., S. Harada, N. Yamamoto, and M. Nakai. 1988. Entry of human immunodeficiency virus (HIV) into MT-2, human T-cell leukemia virus carrier cell line. *Arch. Virol.* **102**:29–38.
- Grewe, C., A. Beck, and H. R. Gelderblom. 1990. HIV: early virus-cell interactions. *J. Acquir. Immune Defic. Syndr.* **3**:965–974.
- He, J., Y. Chen, M. Farzan, H. Choe, A. Ohagen, S. Gartner, J. Busciglio, X. Yang, W. Hofmann, W. Newman, C. R. Mackay, J. Sodroski, and D. Gabuzda. 1997. CCR3 and CCR5 are coreceptors for HIV-1 infection of microglia. *Nature* **385**:645–649.
- Henley, J. R., E. W. Krueger, B. J. Oswald, and M. A. McNiven. 1998. Dynamin-mediated internalization of caveolae. *J. Cell Biol.* **141**:85–99.
- Katen, L. J., M. M. Januszski, W. F. Anderson, K. J. Hasenkrug, and L. H. Evans. 2001. Infectious entry by amphotropic as well as ecotropic murine leukemia viruses occurs through an endocytic pathway. *J. Virol.* **75**:5018–5026.
- Kosaka, T., and K. Ikeda. 1983. Possible temperature-dependent blockage of synaptic vesicle recycling induced by a single gene mutation in *Drosophila*. *J. Neurobiol.* **14**:207–225.
- Kosaka, T., and K. Ikeda. 1983. Reversible blockage of membrane retrieval and endocytosis in the garland cell of the temperature-sensitive mutant of *Drosophila melanogaster*, shibirets1. *J. Cell Biol.* **97**:499–507.
- Koyama, A. H., and T. Uchida. 1987. The mode of entry of herpes simplex virus type 1 into Vero cells. *Microbiol. Immunol.* **31**:123–130.

31. Lee, S., Y. Zhao, and W. F. Anderson. 1999. Receptor-mediated Moloney murine leukemia virus entry can occur independently of the clathrin-coated-pit-mediated endocytic pathway. *J. Virol.* **73**:5994–6005.
32. Lucius, H., T. Friedrichson, T. V. Kurzchalia, and G. R. Lewin. 2003. Identification of caveolae-like structures on the surface of intact cells using scanning force microscopy. *J. Membr. Biol.* **194**:97–108.
33. Marechal, V., F. Clavel, J. M. Heard, and O. Schwartz. 1998. Cytosolic Gag p24 as an index of productive entry of human immunodeficiency virus type 1. *J. Virol.* **72**:2208–2212.
34. Marechal, V., M. C. Prevost, C. Petit, E. Perret, J. M. Heard, and O. Schwartz. 2001. Human immunodeficiency virus type 1 entry into macrophages mediated by macropinocytosis. *J. Virol.* **75**:11166–11177.
35. Marsh, M., and A. Pelchen-Matthews. 2000. Endocytosis in viral replication. *Traffic* **1**:525–532.
36. Matlin, K. S., H. Reggio, A. Helenius, and K. Simons. 1982. Pathway of vesicular stomatitis virus entry leading to infection. *J. Mol. Biol.* **156**:609–631.
37. McClure, M. O., M. Marsh, and R. A. Weiss. 1988. Human immunodeficiency virus infection of CD4-bearing cells occurs by a pH-independent mechanism. *EMBO J.* **7**:513–518.
38. Meier, O., K. Boucke, S. V. Hammer, S. Keller, R. P. Stidwill, S. Hemmi, and U. F. Greber. 2002. Adenovirus triggers macropinocytosis and endosomal leakage together with its clathrin-mediated uptake. *J. Cell Biol.* **158**:1119–1131.
39. Mothes, W., A. L. Boerger, S. Narayan, J. M. Cunningham, and J. A. Young. 2000. Retroviral entry mediated by receptor priming and low pH triggering of an envelope glycoprotein. *Cell* **103**:679–689.
40. Munk, C., S. M. Brandt, G. Lucero, and N. R. Landau. 2002. A dominant block to HIV-1 replication at reverse transcription in simian cells. *Proc. Natl. Acad. Sci. USA* **99**:13843–13848.
41. Nicola, A. V., A. M. McEvoy, and S. E. Straus. 2003. Roles for endocytosis and low pH in herpes simplex virus entry into HeLa and Chinese hamster ovary cells. *J. Virol.* **77**:5324–5332.
42. Ochoa, G. C., V. I. Slepnev, L. Neff, N. Ringstad, K. Takei, L. Daniell, W. Kim, H. Cao, M. McNiven, R. Baron, and P. De Camilli. 2000. A functional link between dynamin and the actin cytoskeleton at podosomes. *J. Cell Biol.* **150**:377–389.
43. Oh, P., D. P. McIntosh, and J. E. Schnitzer. 1998. Dynamin at the neck of caveolae mediates their budding to form transport vesicles by GTP-driven fission from the plasma membrane of endothelium. *J. Cell Biol.* **141**:101–114.
44. Patterson, S., J. S. Oxford, and R. R. Dourmashkin. 1979. Studies on the mechanism of influenza virus entry into cells. *J. Gen. Virol.* **43**:223–229.
45. Pauza, C. D., and T. M. Price. 1988. Human immunodeficiency virus infection of T cells and monocytes proceeds via receptor-mediated endocytosis. *J. Cell Biol.* **107**:959–968.
46. Pelchen-Matthews, A., P. Clapham, and M. Marsh. 1995. Role of CD4 endocytosis in human immunodeficiency virus infection. *J. Virol.* **69**:8164–8168.
47. Pelkmans, L., and A. Helenius. 2003. Insider information: what viruses tell us about endocytosis. *Curr. Opin. Cell Biol.* **15**:414–422.
48. Pelkmans, L., J. Kartenbeck, and A. Helenius. 2001. Caveolar endocytosis of simian virus 40 reveals a new two-step vesicular-transport pathway to the ER. *Nat. Cell Biol.* **3**:473–483.
49. Pelkmans, L., D. Puntener, and A. Helenius. 2002. Local actin polymerization and dynamin recruitment in SV40-induced internalization of caveolae. *Science* **296**:535–539.
50. Perez, L., and L. Carrasco. 1993. Entry of poliovirus into cells does not require a low-pH step. *J. Virol.* **67**:4543–4548.
51. Pierson, T. C., and R. W. Doms. 2003. HIV-1 entry and its inhibition. *Curr. Top. Microbiol. Immunol.* **281**:1–27.
52. Schaeffer, E., V. B. Soros, and W. C. Greene. 2004. Compensatory link between fusion and endocytosis of human immunodeficiency virus type 1 in human CD4 T lymphocytes. *J. Virol.* **78**:1375–1383.
53. Schlunck, G., H. Damke, W. B. Kiesses, N. Rusk, M. H. Symons, C. M. Waterman-Storer, S. L. Schmid, and M. A. Schwartz. 2004. Modulation of Rac localization and function by dynamin. *Mol. Biol. Cell* **15**:256–267.
54. Sever, S., H. Damke, and S. L. Schmid. 2000. Garrotes, springs, ratchets, and whips: putting dynamin models to the test. *Traffic* **1**:385–392.
55. Sieczkarski, S. B., and G. R. Whittaker. 2002. Dissecting virus entry via endocytosis. *J. Gen. Virol.* **83**:1535–1545.
56. Skehel, J. J., P. M. Bayley, E. B. Brown, S. R. Martin, M. D. Waterfield, J. M. White, I. A. Wilson, and D. C. Wiley. 1982. Changes in the conformation of influenza virus hemagglutinin at the pH optimum of virus-mediated membrane fusion. *Proc. Natl. Acad. Sci. USA* **79**:968–972.
57. Sodeik, B. 2000. Mechanisms of viral transport in the cytoplasm. *Trends Microbiol.* **8**:465–472.
58. Stein, B. S., S. D. Gowda, J. D. Lifson, R. C. Penhallow, K. G. Bensch, and E. G. Engleman. 1987. pH-independent HIV entry into CD4-positive T cells via virus envelope fusion to the plasma membrane. *Cell* **49**:659–668.
59. Tobiume, M., J. E. Lineberger, C. A. Lundquist, M. D. Miller, and C. Aiken. 2003. Nef does not affect the efficiency of human immunodeficiency virus type 1 fusion with target cells. *J. Virol.* **77**:10645–10650.
60. van der Blik, A. M., T. E. Redelmeier, H. Damke, E. J. Tisdale, E. M. Meyerowitz, and S. L. Schmid. 1993. Mutations in human dynamin block an intermediate stage in coated vesicle formation. *J. Cell Biol.* **122**:553–563.
61. Welker, R., H. Hohenberg, U. Tessmer, C. Huckhagel, and H. G. Krausslich. 2000. Biochemical and structural analysis of isolated mature cores of human immunodeficiency virus type 1. *J. Virol.* **74**:1168–1177.